# An overview of the ACE-2 CLOUDYCOLUMN closure experiment

J.-L. Brenguier, P. Y. Chuang, Yves Fouquart, D.W. Johnson, Frédéric Parol, Hanna Pawlowska, Jacques Pelon, L. Schüller, F. Schröder, J. R. Snider

*Tellus (2000), 52B, 815–827*
*Printed in UK. All rights reserved*


**TELLUS**
*ISSN 0280–6509*

# An overview of the ACE-2 CLOUDYCOLUMN closure experiment

By J. L. BRENGUIER[1]*, P. Y. CHUANG[2], Y. FOUQUART[3], D. W. JOHNSON[4] F. PAROL[3], HANNA PAWLOWSKA[5]**, JACQUES PELON[6], LOTHAR SCHÜLLER[7], F. SCHRÖDER[8] and J. SNIDER[9] [1]*Météo-France (CNRM/GAME), Toulouse, France,* [2]*California Institute of Technology, Pasadena, California, USA,* [3]*Laboratoire d'Optique Atmosphérique, Université des Sciences et Techniques de Lille, France,* [4]*Met. Research Flight, DERA, Farnborough, UK,* [5]*Laboratoire de Météorologie Dynamique, Paris, France,* [6]*Service d'Aéronomie, Paris, France,* [7]*Institut für Weltraumwissenschaften, Freie Universität Berlin, Germany,* [8]*Deutsches Forschungszentrum für Luft- und Raumfahrt e.V., Wessling, Germany,* [9]*Dept of Atmos. Sciences, University of Wyoming, USA*

(Manuscript received 2 February 1999; in final form 15 October 1999)

ABSTRACT

CLOUDYCOLUMN is one of the 6 ACE-2 projects which took place in June-July 1997, between Portugal and the Canary Islands. It was specifically dedicated to the study of changes of cloud radiative properties resulting from changes in the properties of those aerosols which act as cloud condensation nuclei. This process is also refered to as the aerosol indirect e ect on climate. CLOUDYCOLUMN is focused on the contribution of stratocumulus clouds to that process. In addition to the basic aerosol measurements performed at the ground stations of the ACE-2 project, 5 instrumented aircraft carried out in situ characterization of aerosol physical, chemical and nucleation properties and cloud dynamical and microphysical properties. Cloud radiative properties were also measured remotely with radiometers and a lidar. 11 case studies have been documented, from pure marine to significantly polluted air masses. The simultaneity of the measurements with the multi-aircraft approach provides a unique data set for closure experiments on the aerosol indirect e ect. In particular CLOUDYCOLUMN provided the 1st experimental evidence of the existence of the indirect e ect in boundary layer clouds forming in polluted continental outbreacks. This paper describes the objectives of the project, the instrumental setup and the sampling strategy. Preliminary results published in additional papers are briefly summarized.

## 1. Introduction and scientific background

CLOUDYCOLUMN was one of the 6 field projects in ACE-2 (Raes et al., 2000). It was specifically dedicated to the study of the indirect e ect of aerosols on climate. "Indirect e ect" refers here to changes of cloud radiative properties resulting from changes in the properties of those aerosols which act as cloud condensation nuclei (CCN). Changes in chemical composition or physical properties of CCN has the potential to induce changes in cloud droplet number concentration. 2 e ects are recognised. For a given liquid water content (LWC) a cloud made of numerous small droplets is brighter (higher albedo) than a cloud made of a few big droplets. This 1st e ect is also known as the Twomey e ect (Twomey, 1977).

* Corresponding author
METEO-FRANCE, CNRM, GMEI/MNP, 42 av. Coriolis, 31057 Toulouse Cedex 01, France.
e-mail: jlb@meteo.fr
** On leave from Institute of Geophysics, University of Warsaw, Poland.

Polluted clouds are also less e cient at producing precipitation, resulting in an increase of cloud lifetime and horizontal extent (Albrecht, 1989).

The 1995 IPCC report (Houghton et al., 1995) draws together recent study results which show that the current estimate of the global mean radiative forcing due to anthropogenic aerosols, although highly uncertain, is of a comparable magnitude but opposite in sign to the forcing due to anthropogenic greenhouse gases. For the direct e ect the IPCC report gives a best estimate of $-0.5$ W/m$^2$ (range $-0.2$ to $-1.5$ W/m$^2$) for the e ect of aerosol on the global radiation balance. No best estimate is given for the indirect e ect, only an uncertainty range of 0 to $-1.5$ W/m$^2$. Thus the authors of the IPCC report consider the net e ect is a cooling of the climate system, with the main contribution coming from marine boundary layer clouds. The high albedos (30–40%) of these clouds compared with the ocean background (10%) give rise to large deficits in the absorbed solar radiative flux at the top of the atmosphere, while their low altitude prevents significant compensation in thermal emission (Randall et al., 1984).

Although "indirect e ects" have been implicitly accepted in the di erence between marine and continental clouds for some decades, few experiments have been able to qualify these e ects in individual cloud systems. Examples are the ship track studies o the west coast of the USA (King et al., 1993) and, at a larger scale, the di erence in radiative properties between summer and winter clouds o the coast of Australia, that are attributed to changes in the natural CCN concentration (Boers et al., 1998).

One di culty with in situ studies arises from the dependence of the radiative properties of a cloud on its morphological properties (particularly geometrical thickness), whereas the e ect of anthropogenic aerosols through changes in droplet concentration is a second order e ect. In the Twomey approximation (plane parallel cloud vertically uniform), the optical thickness varies with cloud geometrical thickness $H$ and the cube root of droplet concentration $N^{1/3}$ (Twomey, 1977):

$$\tau \propto N^{1/3} H. \quad (1)$$

For a cloud with an adiabatic vertical profile of LWC, a more realistic description, the optical thickness is proportional to the power 5/3 of the geometrical thickness (Boers and Mitchell, 1994; Brenguier et al., 2000):

$$\tau \propto N^{1/3} H^{5/3}. \quad (2)$$

The 2nd indirect e ect is related to changes in cloud precipitation e ciency. At a fixed LWC value, an increase of the droplet concentration results in a decrease of the droplet sizes and a reduced probability of collision-coalescence between droplets to form precipitation (Albrecht, 1989). It is thus likely that an increase of the droplet concentration will result in a decrease of the precipitation e ciency and therefore in an increase of the cloud spatial extent and lifetime, hence an increase of mean cloud albedo. The higher dependence of optical thickness on geometrical thickness ($H^{5/3}$ instead of $H$) is important because it suggests that the second indirect e ect could be more significant than the first.

The experimental assessment of the indirect e ect is challenging because of the high variability of the cloud morphological characteristics whereas changes in the droplet concentration that are related to changes of the CCN population are rather limited. Radiative properties observed in a cloud system are also highly variable with a standard deviation of the same order of magnitude as the change expected between a pure marine cloud and a polluted one. Droplet number concentration is also highly variable (Pawlowska and Brenguier, 2000). Although values observed near cloud base in convective updrafts closely reflect the CCN population, these conditions represent a limited fraction of the cloud systems. In other regions the droplet concentration is a ected by entrainment and mixing with sub-saturated air and by the formation of precipitation.

A careful experimental design is essential to establish a direct link between CCN properties, droplet number concentration and cloud radiative properties. The methodology used in CLOUDYCOLUMN to examine both aspects of the indirect e ect was designed to overcome these di culties. In situ measurements of the cloud microphysics were synchronized with simultaneous measurements of the cloud radiative properties made by a second aircraft flying above the cloud layer. Data obtained in this manner have been particularly useful for the validation of the anticipated relationship between optical and cloud geometrical thickness (Brenguier et al., 2000).

Furthermore, cloud systems with similar morphologies but which were fed by air with di erent aerosol properties were studied, with emphasis on thin stratocumulus cloud systems. This is because the radiative properties of thin clouds are the most sensitive to a change in the droplet concentration. In addition, to avoid sampling artifacts, identical sampling strategies were used in the various cases studied. Finally, the flight track used for most missions (60 km square) allowed retrieval of turbulent fluxes in the boundary layer.

## 2. The instrumental setup

The instrumental setup during the CLOUDYCOLUMN field experiment included 5 instrumented aircraft (Fig. 1).

- The MRF C-130 was equipped for measurements of the physical, chemical and nucleation properties of the aerosols, and for measurements of the turbulent fluxes and cloud microphysics. The complete description of the C-130 equipment is given in Johnson et al. (2000).
- The Pelican is operated by the Center for Interdisciplinary Remotely Piloted Aircraft Studies (CIRPAS). The Pelican, a highly modified Cessna Skymaster, although significantly smaller than the C-130, was also equipped for measurement of aerosol properties and turbulent fluxes. A complete description of the CIRPAS Pelican equipment is given in Raes et al. (2000). Chemical composition measurements were conducted for some CLOUDYCOLUMN flights and provide a single measurement of average boundary layer sulfate, nitrate, chloride, organic carbon and trace metal concentrations (Schmeling et al., 2000).

These 2 aircraft were dedicated to boundary layer measurements.

- The Météo-France M-IV was equipped for microphysical measurements of aerosols, cloud droplets, precipitation, aerosol physical and nucleation properties, and turbulent fluxes.
- The DLR Do-228 carried a multiwavelength radiometer (FUB-OVID), a multidirectional radiometer (LOA-POLDER) and a scanning radiometer (FUB-CASI).
- The ARAT F-27 participated in the field experiment for a short period with its airborne lidar (SA-LEANDRE).

These latter 2 aircraft carried out remote measurements of the cloud radiative properties. In addition to these aircraft measurements, information on the properties of aerosols was obtained at the ACE-2 ground stations in Portugal, Madeiras, Canaries and Azores (see Heintzenberg and Russell, 2000).

Details on the instrumentation of the M-IV,

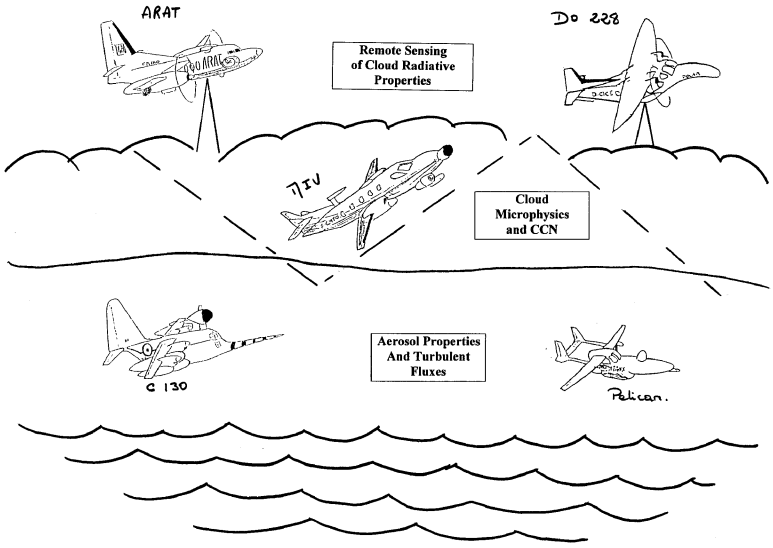


*Fig. 1.* Illustration of the CLOUDYCOLUMN experiment.

Do-228 and ARAT aircraft are given in the following sections.

### 2.1. Instrumentation on board the M-IV

Sampling characteristics of the aerosol instrumentation flown on the M-IV during ACE-2 are summarized in Figs. 2 and 3. Four instruments, 2 condensation nuclei (CN) counters (TSI 3760A; Schröder and Ström, 1997), the PCASP-100X (Petzold et al., 1997), and the University of Wyoming cloud condensation nucleus counter (WYO-CCN; Snider and Brenguier, 2000) were located inside the M-IV and sampled aerosol via 2 separate inlets. The CCN were sampled via a quasi-isokinetic inlet which was located within a velocity di user. The 3 other aerosol instruments sampled via a reverse-flow inlet similar to the device characterized by Schröder and Ström (1997). The upper cut-o diameters were estimated to be 8 μm and 1 μm, respectively (Snider and Brenguier, 2000). The former is a semi-quantitative assessment and because of non-ideal e ects discussed by Huebert et al. (1990) it probably overestimates the actual size cut.

In addition, the M-IV instrumentation included three optical spectrometers for the characterization of larger aerosol (FSSP-300; Baumgardner et al., 1992), droplets (Fast-FSSP; Brenguier et al., 1998), and precipitation (OAP 200-X, PMS Inc, Boulder, Colorado, USA). These devices were mounted on the fuselage below the cockpit. The M-IV was also equipped for the measurements of wind, thermodynamics, broad-band radiation, and turbulent fluxes.

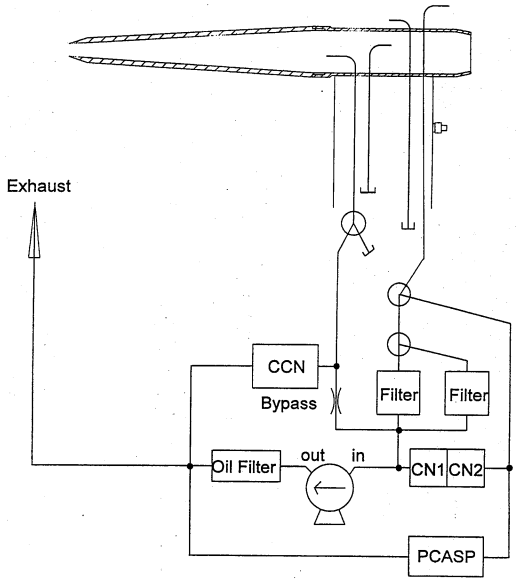


*Fig. 2.* Aerosol sampling system implemented on the MERLIN aircraft.

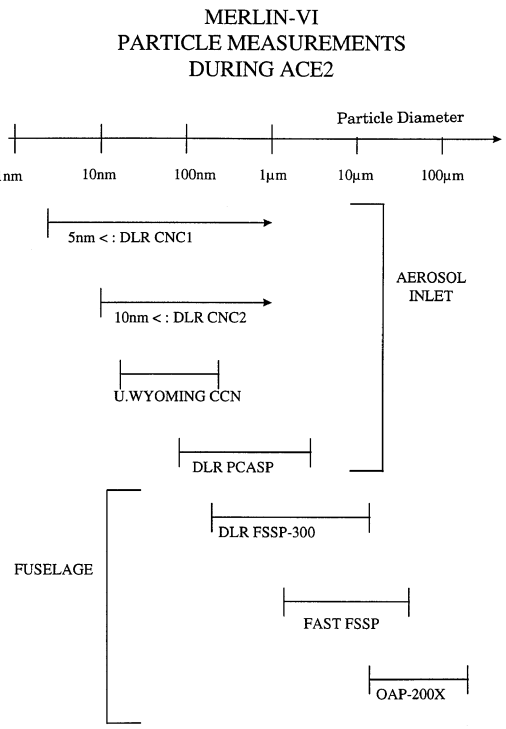


*Fig. 3.* Summary of the particle measurement capability on board the M-IV. *Aerosol inlet* refers to instruments installed inside the aircraft and connected to the aerosol inlet, thus measuring dry aerosols. *Fuselage* refers to instruments mounted on the aircraft nose, thus measuring the aerosols and cloud particles at ambient humidity.

### 2.2. Radiative measurements on board the Do-228

The Do-228 was equipped with three radiometers. POLDER is a multidirectional radiometer in the visible, operated by the Laboratoire d'Optique Atmospherique (Lille, France). The instrument and preliminary results are described in Parol et al. (2000). A similar instrument was installed on the ADEOS satellite and provided measurements for the first week of the experiment.

The Optical Visible and Near Infrared Detector (OVID) is a high resolution multichannel analyzer for airborne remote sensing of atmospheric properties in the spectral range of 500 nm to 1700 nm (Schüller et al., 1997). The instrument consists of two separate, but nearly identical detection systems. During the ACE 2 field campaign, the OVID performed radiance measurements of the reflected solar radiation in a nadir viewing configuration, with a spectral resolution of 0.8 nm between 700 nm and 1000 nm (OVID-VIS) and 6 nm between 1000 nm and 1700 nm (OVID-NIR). The sampling time of both systems was about 100 ms during the ACE 2 flights above clouds. The combination of non-absorbing shortwave channels and near infrared channel within absorbtion bands of liquid water (1500 nm) enables the remote sensing of cloud optical and microphysical properties. Channels within absorption bands can be used to determine cloud top heights ($O_2$-A band at 760 nm) and atmospheric water vapour content ($\rho\sigma\tau$ band at 900 nm).

The Compact Airborne Spectrographic Imager (CASI) (Babey and So er, 1992) is a "pushbroom" imaging spectrometer with a 34° field of view (across track). The spectral range from 430 nm to 870 nm can be covered with 512 pixels in the spatial axis and 288 spectral channels. During the ACE 2 campaign, CASI was operated onboard the Do-228 aircraft to measure reflected solar radiation. The programmable channels were chosen to allow derivation of cloud albedo and optical thickness (with maximum spatial resolution) as well as cloud top height, using measurements within the $O_2$-A band over 39 directions.

### *2.3. Lidar measurements on board the ARAT*

The French Atmospheric and Remote sensing Aircraft (ARAT) took part in the Cloudy Column experiment after the first continental aerosol outbreak was observed from the south of Portugal. It was flown with the airborne lidar LEANDRE2 (Flamant et al., 1998), which was operating at 730 nm. The lidar measurements allowed retrieval of the cloud top height and the in-cloud extinction near cloud top. Updrafts and downdrafts were identified from cloud-top height variations. The altitude of the cloud base has been obtained in some of the downdrafts, where the optical thickness was less than 3, allowing the lidar beam to penetrate the cloud down to the surface. Lidar data were taken simultaneously with upward and downward shortwave and longwave flux measurements from Eppley pyranometers and pyrgeometers.

## 3. Summary of the field campaign

The meteorological conditions during the ACE-2 experiment are presented in Raes et al. (2000). CLOUDYCOLUMN performed experiments during the 1st and 2nd ACE-2 pollution events (7–9 July and 17–19 July, respectively) and in the clean periods before these events. The list of the flights is reported in Table 1. With the exception of problems with the PCASP (17 June–16 July) and POLDER (8 July), all instrumentation functioned throughout the campaign. The ARAT aircraft with the LEANDRE lidar only participated in the experiment on 8, 9 July.

## 4. Sampling strategy

As indicated in Table 1, most flights were performed along a square flight-track; the typical horizontal dimension was 60 km. The M-IV was flown either at constant altitude (in cloud or below cloud), or along a zig-zag track that extended from above to below the cloud layer. The Do-228 was flown about 1 km above cloud top. These two aircraft were synchronized by maintaining the M-IV within the field of view of the Do-228 radiometers, with an accuracy of 100 m.

Data acquired from the constant-altitude legs were used to characterize the CCN activation and aerosol spectra (below cloud), droplet and drizzle distributions (in cloud), and turbulent fluxes (all legs). The zig-zag legs provide a rapid characterization of cloud base and top altitudes and of the vertical profile of the microphysics. The distance flown by the M-IV for a complete traverse of the layer ranges between 5 and 10 km depending on the cloud geometrical thickness.

The third aircraft, either the C-130 or the Pelican, was flown in the boundary layer below cloud base (except for flights on 25 June and 8 and 17 July). For flight safety reasons the third aircraft was positioned across the square from the

Table 1. *CLOUDYCOLUMN flights summary*

| Date | Boundary layer | In situ | Remote sensing | Air mass | Flight description |
|---|---|---|---|---|---|
| 17 Jun | | M-IV | | | spectrometer tests |
| 19 Jun | | M-IV | | | spectrometer tests |
| 21 Jun | | M-IV | | | spectrometer tests |
| 24 Jun | | M-IV | | | spectrometer tests |
| 25 Jun | | M-IV | Do-228 | marine | square* |
| 26 Jun | C-130 | M-IV | Do-228 | marine | square |
| 01 Jul | | M-IV | | | intercalibration |
| 04 Jul | Pelican | M-IV | Do-228 | marine | square |
| 05 Jul | Pelican | M-IV | | marine | square |
| 07 Jul | Pelican | M-IV | Do-228 | polluted | long legs |
| 08 Jul | | M-IV | Do-228 | | transit to Porto-Santo |
| 08 Jul | | M-IV | Do-228/ARAT | polluted | long legs |
| 08 Jul | | M-IV | Do-228 | | transit to Tenerife |
| 09 Jul | Pelican | M-IV | Do-228/ARAT | polluted | square |
| 16 Jul | C-130/Pelican | M-IV | Do-228 | marine | square |
| 16 Jul | | M-IV | Do-228 | | transit to Tenerife |
| 17 Jul | | M-IV | Do-228 | polluted | square |
| 18 Jul | Pelican | M-IV | Do-228 | polluted | square |
| 19 Jul | C-130/Pelican | M-IV | Do-228 | polluted | square |
| 21 Jul | | M-IV | Do-228 | | intercalibration |
| 07/22 | | M-IV | Do-228 | | intercalibration |

* "Square" refers to 60 km side square figures flown by the aircraft below, inside, and above the cloud layer, as shown in Fig. 4.

M-IV. The delay between the two aircraft was less than 30 min. Close synchronization between the M-IV and the C-130/Pelican was not as important as between the M-IV and the Do-228 because the aerosol was distributed homogeneously within the boundary layer. But on 19 July, a significant trend in aerosol concentrations was observed between the southern and the northern extent of the square. On this day, both the Pelican and the C-130 conducted boundary layer measurements, with the Pelican flying an octogonal pattern $\approx 100$ km upwind of the 60 km square. The spatial inhomogeneity of the aerosol distributions is thus well described in this case.

Fig. 4 shows AVHRR derived cloud images from both a clean and a polluted CLOUDYCOLUMN experiments. The bottom figures represent a large view of the Eastern-Atlantic area and the top figures show the local region of the Canary Islands, with the aircraft trajectory superimposed. The cloud systems in these two days look similar morphologically, although microphysical and radiative measurements demonstrate that their properties are quite di erent. Fig. 5 shows a typical M-IV trajectory, with horizontal sampling below and inside cloud, and a series of ascents and descents throughout the layer. Each of these ascents or descents provides an estimation of the typical droplet concentration $N$ and of the cloud geometrical thickness $H$ at the location of the traverse. The whole campaign is summarized in Fig. 6 where each point corresponds to one of the vertical profiles. Eight flights are reported in the figure. The two most marine cases are characterized by droplet number concentrations lower than 100 $cm^{-3}$ and cloud geometrical thickness up to 350 m. The other flights show more or less polluted conditions with droplet number concentration up to 400 $cm^{-3}$ on 9 July. The geometrical thickness is slightly lower for the polluted cases. This could be related to the observation that polluted air was also dryer than marine air. CLOUDYCOLUMN experiments generally were conducted at the end of pollution outbreaks over the region, when the influence of continental air was declining. Isolines in Fig. 6 illustrate how various cases could be classified in term of optical thickness and e ective radius. For example, it can be seen that an e ective radius of about 9 μm is representative of either a

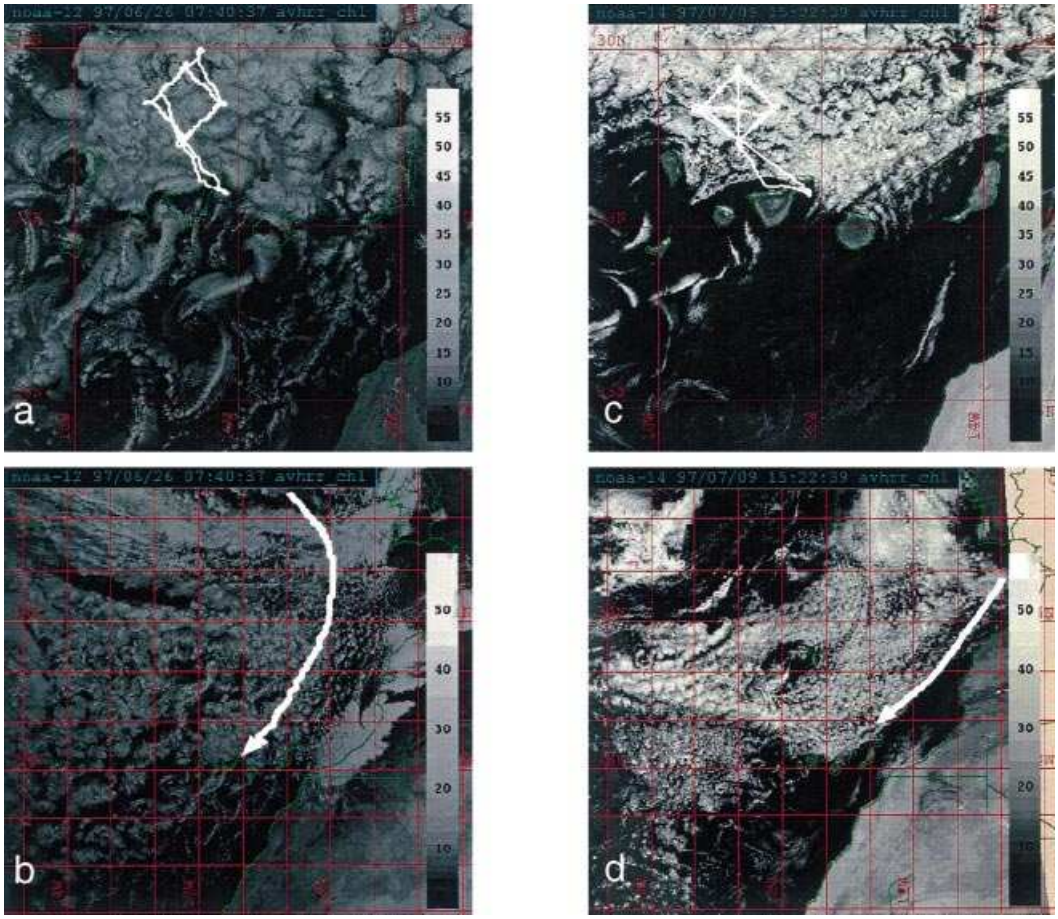


*Fig. 4.* AVHRR visible channel images for the 26 June (a) and (b), and the 9 July (c) and (d) cases; detailed view of the sampling area (Canary Islands, 13–19W, 25.5–30.5N) in (a) and (c), with the aircraft track superimposed; large view of the North-East Atlantic region (6–26W, 22–40N) in (b) and (d), with the trajectory of the air mass in the boundary layer superimposed.

thin marine cloud or a thick polluted one. Hence, the droplet e ective radius is not a particularly good parameter for detecting the anthropogenic aerosol e ects on clouds, if cloud geometrical thickness or the liquid water path are not measured concomitantly. On the other hand, droplet concentration is a good parameter for characterizing the air mass type.

## 5. Scientific analysis

The ultimate objective of the CLOUDY-COLUMN project is to develop a reliable parameterization of the indirect e ect in marine boundary layer clouds. The primary steps have been designed as partial closure experiments. They are briefly described in this section.

### 5.1. Cloud base

The 1st step in a climate model, for the simulation of the indirect e ect, is to predict the physical and chemical properties of the aerosols in the atmosphere, their sources, transport, transformations and sinks. The 2nd step is to derive from these properties the probability distribution of the droplet number concentration in clouds, as a

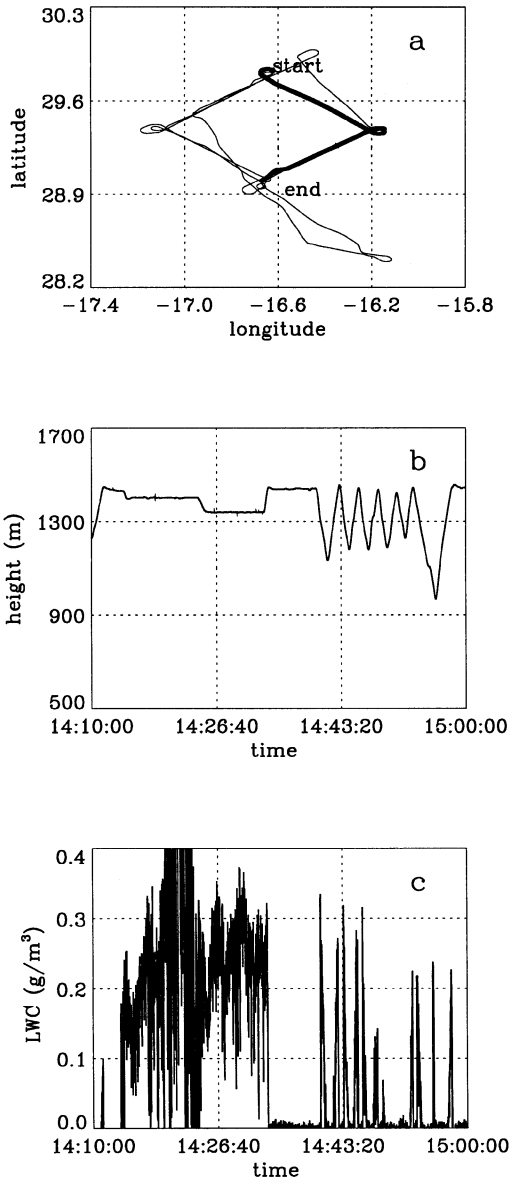


*Fig. 5.* M-IV flight on 26 June 1997: (a) horizontal trajectory; (b) altitude versus time for the flight section indicated by a thick line in (a); (c) same as (b) for LWC.

function of the probability distribution of vertical speed at the cloud base. Cloud base closure in CLOUDYCOLUMN consists in the comparison between values of droplet number concentration measured in cloud with the values derived from the activation model initialized with the measured aerosol distributions and vertical velocity. With measurements of CCN activation spectra it is also possible to proceed in 2 steps. The first closure involves the comparison of the measured CCN activation spectra with those derived from the measured aerosol properties and the Köhler theory. The work of Chuang et al. and Wood et al. (2000) shows that predicted CCN concentrations are substantially larger than the direct observations. Further analysis and intercomparisons using laboratory aerosols will be needed to identify the source of this discrepancy.

Closure was also evaluated between the measured droplet concentration and the value derived from measured CCN activation spectra and vertical velocity. Two approaches can be tested:

(i) *Single updraft closure.* It is possible from aircraft measurements to characterize the vertical velocity and the droplet number concentration within convective updrafts. Closure is evaluated between the measured concentration and the one predicted with the models or parameterizations initialized with the measured CCN activation spectrum and the measured vertical velocity.

(ii) *Statistical updraft closure.* There is a serious limitation in the approach described above because it must be assumed that the vertical velocity measured inside the cloud, at a level where droplets are detectable, that is about 100 m above the activation level, correctly characterizes the velocity the parcel has experienced from below cloud base up to the observation level. Alternatively, the frequency distribution of the vertical velocity can be derived from horizontal legs at the cloud base. The frequency distribution of the predicted concentration is then derived from the CCN properties measured below cloud base and from the frequency distribution of vertical velocity. For closure it is compared to the frequency distribution of the droplet number concentration measured higher in the cloud.

This is the approach tested by Snider and Brenguier (2000). These authors show that the degree of consistency between measured and predicted values of droplet concentration is within a factor of two over a broad range extending from 20 to 400 $cm^{-3}$. This result is encouraging but does not provide the link between aerosol physicochemical properties and droplet concentration needed for GCM simulations. Continued analysis

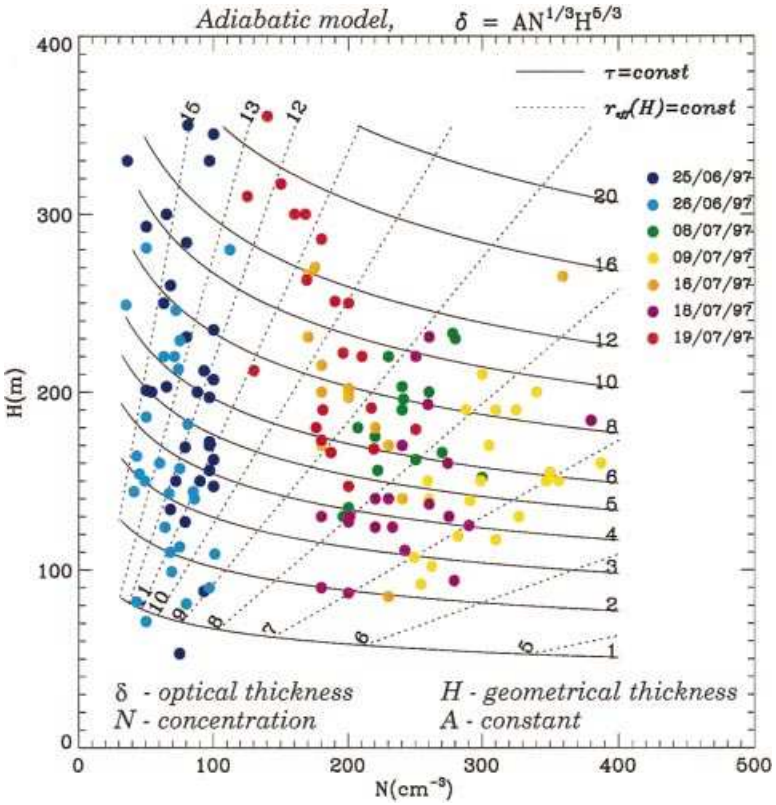


*Fig. 6.* Summary of cloud droplet number concentrations and cloud geometrical thicknesses measured by the M-IV during eight flights of the ACE-2 campaign. Each dot corresponds to values measured during either an ascent or a descent throughout the cloud layer. The superimposed isolines are the e ective radius at the top of the cloud layer and the optical thickness, as derived from the adiabatic model with the corresponding geometrical thickness and droplet number concentration.

is needed to identify the most important aerosol and meteorological properties that are necessary for describing the indirect e ect in climate models.

### 5.2. *Cloud depth*

An actual cloud is far from the idealized plane parallel model that has been used extensively for radiation calculations (Slingo and Schrecker, 1982). In such a model the cloud microphysical properties are assumed to be uniform horizontally and vertically. Vertical uniformity implies that the cloud optical thickness $\tau$ is proportional to the geometrical thickness $H$ (Twomey, 1977). But, for convective updraft, the broad structure observed is that the liquid water content increases linearly with altitude above cloud base, droplet number concentration is constant and the droplet mean volume diameter increases as $H^{1/3}$. Although values of the microphysical parameters are always smaller than the adiabatic prediction, the adiabatic model provides a more realistic description of the vertical profiles of microphysics than the vertically uniform model. The resulting higher sensitivity to $H$ implies that changes in the cloud morphology due to the e ects of aerosols on precipitation e ciency might induce cloud albedo modifications exceeding the first indirect e ect.

The partial closure here is concerned with the characterization of the vertical profiles of microphysics compared to the profile predicted with an adiabatic parcel model. The zig-zag legs are particularly suited for such an analysis. The observations presented in Brenguier et al. (2000) and in

Pawlowska and Brenguier (2000) show that most of the observed profiles are close to the adiabatic model, thus validating this model for radiative transfer calculations.

### 5.3. Single cloud albedo

The next step consists in the validation of the radiative transfer calculation throughout a vertically stratified cloud at the scale of a stratocumulus cell. Such a local closure experiment was possible in CLOUDYCOLUMN because of the close synchronization between in-cloud measurements of the vertical profile of the microphysics and the remote sensing measurements of the cloud radiative properties. Comparisons between the values of optical thickness derived from OVID measurements and the values calculated with the adiabatic parameterization initialized with the measured $H$ and $N$ are presented in Brenguier et al. (2000). They clearly demonstrate proportionality between optical thickness and $H^{5/3}$ rather than $H$. The adiabatic parameterization provides a way of deriving $H$ and $N$ from the measured reflectances in the visible and near infra-red (Fig. 7), with a method similar to the ones developed by Twomey and Cocks (1989) or Nakajima and King (1990) for the retrieval of $\tau$ and the e ective droplet diameter, using the plane-parallel model. The analysis of the ACE-2 cases shows that the derived values of the droplet number concentration ($100\ cm^{-3}$ in polluted and $25\ cm^{-3}$ in clean) are always underestimated with respect to the measured values ($244\ cm^{-3}$ in polluted and $55\ cm^{-3}$ in clean). Such a discrepancy, similar to the overestimation of the values of droplet e ective diameter retrieved with the plane-parallel model, has been often attributed to anomalous absorption (Twomey and Cocks, 1989; Stephens and Tsay, 1990).

The single cloud albedo closure experiment thus demonstrates that the adiabatic model is more realistic than the plane-parallel model for the parameterization of the cloud radiative properties, but also that the main discrepancy between measured and predicted values of cloud reflectances still remains unexplained.

### 5.4. Cloud system albedo

The last step is to provide parameterization at the scale of a climate model grid, that is at a scale of 100 km. In the plane-parallel model it has also been assumed that cloud properties are uniform horizontally. In fact actual clouds are inhomogeneous with regions of stratocumulus convection, where the adiabatic model is appropriate, and regions a ected by mixing with the dry overlying air and by drizzle formation, where the microphysical properties are sub-adiabatic. Various numerical studies have been performed to evaluate the sensitivity of radiative transfer calculations to cloud inhomogeneities (Barker, 1992; Cahalan et al., 1994a, b; Cahalan et al., 1995; Davis et al., 1996; Duda et al., 1996; Barker, 1996). In particular, it has been demonstrated that the horizontal distribution of the cloud microphysical properties is important to account for the radiative e ect of real stratocumulus systems. These e ects are commonly referred to as the inhomogeneous cloud bias.

Closure at the scale of a cloud system thus consists in the characterization of the turbulent structure of the boundary-layer, of the related statistics of cloud microphysical parameters and of its influence on the mean cloud albedo. This step also includes a study of the consistency between close radiative measurements on board the Do-228 and radiative measurements performed with POLDER on the ADEOS satellite. The M-IV horizontal legs are particularly suited for this approach. Preliminary results are presented in Pawlowska and Brenguier (2000), for the frequency distribution of the microphysical parameters. Further analysis is required to document the scale distribution of the inhomogeneities which is important for the calculation of the inhomogeneous cloud bias. The parameterization of the radiative properties of inhomogeneous cloud systems is a challenge. However, measurements of the cloud reflectances in the visible and near infrared performed during the CLOUDYCOLUMN experiment show clearly that the di erence between clean and polluted clouds is quite significant. Fig. 7 shows the comparison of the distributions of measured reflectances for the 26 June and the 9 July case studies. The contour plots of all the values measured with a horizontal resolution of 100 m over each complete flight are clearly distinct. The isolines represent the values of droplet number concentration and cloud geometrical thickness of an adiabatic cloud with the corresponding values of reflectances at the two wave-

lengths (Brenguier et al., 2000). The measured reflectances are distributed along the 100 $cm^{-3}$ $N$ isoline for the polluted case, and along the 25 $cm^{-3}$ $N$ isoline for the marine case. In situ measurements (Pawlowska and Brenguier, 2000) show distributions of the droplet number concentration centered at 244 $cm^{-3}$ and 55 $cm^{-3}$ for the polluted and marine cases respectively. This illustrates the underestimation of the retrieved droplet concentration mentioned in the previous section, but the ratio between the droplet concentrations of the polluted and the clean cases, which is of the order of 4, is correctly reproduced. This observation can be considered as an experimental evidence of the indirect e ect at the scale of a cloud system.

## 6. Conclusion

CLOUDYCOLUMN is the most recent field experiment where it has been possible to perform simultaneous measurements of aerosol properties, cloud microphysics and cloud radiative properties, in marine stratocumulus. Up to 4 instrumented aircraft were used to sample the same cloud system, with special emphasis on the synchronization between microphysical and radiative measurements. Eleven cases have been documented, with two particularly clean conditions (25, 26 June) and one case of heavy pollution (9 July). The redundancy of the measurements for critical parameters, such as aerosol physical and chemical properties, and CCN activation spectrum, or cloud reflectances measured with multidirectional radiometers, and multiwavelength radiometers, provides a robust data set. Aerosol/microphysics and microphysics/radiation interactions at the scale of the convective cells have been analyzed and important results have already been obtained.

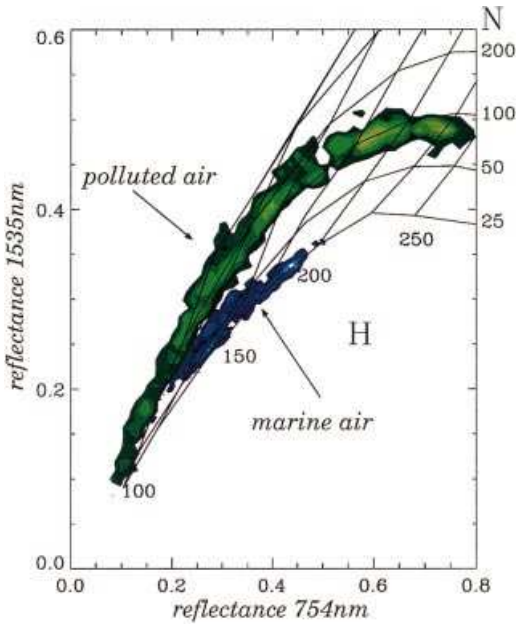


*Fig. 7.* Isocontour of measured cloud reflectances in the visible (754 nm) and near infra-red (1535 nm) with OVID, on 26 June (blue) and 9 July (green). Isolines represent cloud geometrical thickness and droplet number concentration, producing the corresponding cloud reflectances with radiative transfer calculations in an adiabatic cloud model.

Consistency has been tested between aerosol properties and CCN activation spectrum (Chuang et al.; Wood et al., 2000), and between CCN activation spectrum and the droplet concentration by way of the measured vertical velocity (Snider and Brenguier, 2000). These tests have revealed a discordant comparison between predicted and observed CCN number densities. Also documented is an acceptable closure between measurements of CCN, updraft, and cloud droplets. The former result is disapointing since closure between aerosols and CCN is needed to better constrain GCM predictions of the indirect e ect. The disparity should inspire future intercomparisons of CCN and aerosol measurement systems. Modeling work is also needed to improve methodologies used to incorporate bulk chemistry, hygroscopicity, and surface tension data into Köhler theory.

The comparison between values of optical thickness derived from in situ measurements of cloud geometrical thickness and droplet concentration, and values derived from remote sensing measurements of cloud reflectances have demonstrated that the optical thickness is proportional to $H^{5/3}$ instead of $H$, thus validating the adiabatic model of cloud vertical profile for parameterizations of the optical thickness (Brenguier et al., 2000). This result is important because it suggests that the second indirect e ect (precipitation e ciency) could be more significant than the first indirect e ect (Twomey e ect). With the simultaneity of in situ and remote sensing measurements, it has also been possible to check that the significant

di erence between the distributions of the measured reflectances in the visible and near infra-red, between a clean and a polluted case, is not due to di erences in the cloud morphology, but only due to changes in droplet concentration. This provides clear evidence of the indirect e ect of aerosols at the scale of a cloud system. The analysis is now being extended to larger scales and reliable parameterizations of the indirect e ect for climate models are anticipated.

## 7. Acknowledgements

The authors acknowledge the contributions of the ACE-2 participants. This work has been supported by the European Union under grant ENV4-CT95-0117 and by the a liation laboratories and administrations of the authors.

## REFERENCES

Albrecht, B. A. 1989. Aerosols, cloud microphysics, and fractional cloudiness. *Science* **245**, 1227–1230.

Babey, S. K. and So er, R. J. 1992. Radiometric calibration of the compact airborne spectrographic imager (CASI). *Canadian Journal of Remote Sensing* **18**, 233–242.

Barker, H. W. 1992. Solar radiative transfer through clouds possessing isotropic variable extinction coe - cient. *Quart. J. Roy. Meteor. Soc.* **118**, 1145–1162.

Barker, H. W. 1996. Estimating cloud field albedo using one-dimensional series of optical depth. *J. Atmos. Sci.* **53**, 2826–2837.

Baumgardner, D., Dye, J. E., Gandrud, B. W. and Knollenberg, R. G. 1992. Interpretation of measurements made by the forward scattering spectrometer probe (FSSP-300) during the Airborne Arctic Stratospheric Expedition. *J. Geoph. Rev.* **97**, 8035–8046.

Boers, R. and Mitchell, R. M. 1994. Absorption feedback in stratocumulus clouds: influence on cloud top albedo. *Tellus* **46A**, 229–241.

Boers, R., Jensen, J. B. and Krummel, P. B. 1998. Microphysical and short-wave radiative structure of stratocumulus clouds over the Southern Ocean: Summer results and seasonal di erences. *Quart. J. Roy. Meteor. Soc.* **124**, 151–168.

Brenguier, J. L., Bourrianne, T., Coelho, A., Isbert, J., Peytavi, R., Trevarin, D. and Wechsler, P. 1998. Improvements of droplet size distribution measurements with the Fast-FSSP. *J. Atmos. Oceanic. Technol* **15**, 1077–1090.

Brenguier, J. L., Pawlowska, H., Schüller, L., Preusker, R., Fischer, J. and Fouquart, Y. 2000. Radiative properties of boundary layer clouds: droplet e ective radius versus number concentration. *J. Atmos. Sci.* in press.

Cahalan, R. F., Ridgway, W., Wiscombe, J. W. and Bell, T. L. 1994a. The albedo of fractal stratocumulus clouds. *J. Atmos. Sci.* **51**, 2434–2455.

Cahalan, R. F., Ridgway, W. and Wiscombe, J. W. 1994b. Independent pixel and Monte Carlo estimates of stratocumulus albedo. *J. Atmos. Sci.* **51**, 3776–3790.

Cahalan, R. F., Silberstein, D. and Snider, J. B. 1995. Liquid water path and plane-parallel albedo bias during ASTEX. *J. Atmos. Sci.* **52**, 3002–3012.

Chuang, P. Y., Collins, D. R., Pawlowska, H., Snider, J., Jonsson, H. H., Brenguier, J. L., Flagan, R. C. and Seinfeld, J. H. 2000. CCN measurements during ACE-2 and their relationship to cloud microphysical properties. *Tellus* **52B**, 843–867.

Davis, A., Marshak, A., Wiscombe, J. W. and Cahalan, R. 1996. Scale invariance of liquid water distributions in marine stratocumulus. Part I: spectral properties and stationarity issues. *J. Atmos. Sci.* **53**, 1538–1558.

Duda, D. P., Stephens, G. L., Stevens, B. and Cotton, W. R. 1996. E ects of aerosols and horizontal inhomogeneity on the broadband albedo of marine stratus: numerical simulations. *J. Atmos. Sci.* **53**, 3757–3769.

Flamant, C., Trouillet, V., Chazette, P. and Pelon, J. 1998. Wind speed dependence of atmospheric boundary layer optical properties and ocean surface reflectance as observed by airborne backscatter lidar. *J. Geophys. Res.* **103**, 25 137–25 258.

Russell, P. B. and Heintzenberg, J. 2000. An overview of the ACE-2 Clear Sky Column Closure Experiment (CLEARCOLUMN). *Tellus* **52B**, 463–483.

Houghton, J. T., Meira Filho, L. G., Callander, B. A., Harris, N., Kattenberg, A. and Maskell, K. 1995. IPCC 95: Climate change 1995: The science of climate change. Contribution of WG1 to the 2nd Assessment Report of the Intergovernmental Panel on Climate Change, Cambridge Univ. Press.

Huebert, B. J., Lee, G. L. and Warren, W. L. 1990. Airborne aerosol inlet passing e ciency measurements. *J. Geophys. Res.* **95**, 16 369–16 381.

Johnson, D. W., Osborne, S., Wood, R., Suhre, K., Johnson, R., Businger, S., Quinn, P. K., Durkee, P. A., Russell, L. M., Andreae, M. O., O'Dowd, C., Noone, K., Bandy, B., Rudolph, J. and Rapsomanikis, S. 2000. An overview of the Lagrangian Experiments undertaken during the North Atlantic Regional Aerosol Characterisation Experiment (ACE-2). *Tellus* **52B**, 290–320.

King, M. D., Radke, L. F. and Hobbs, P. V. 1993. Optical properties of marine stratocumulus clouds modified by ships. *J. Geoph. Res.* **98**, 2729–2739.

Nakajima, T. and King, M. D. 1990. Determination of the optical thickness and e ective particle radius of

clouds from reflected solar radiation measurements. Part I: theory. *J. Atmos. Sci.* **47**, 1878–1893.

Parol, F., Descloitres, J. and Fouquart, Y. 2000. Cloud optical thickness and albedo retrievals from bidirectional reflectance measurements of POLDER instruments during ACE-2. *Tellus* **52B**, 888–908.

Pawlowska, H. and Brenguier, J. L. 2000. Microphysical properties of stratocumulus clouds during ACE-2. *Tellus* **B**, this issue.

Petzold A., Busen, R., Schröder, F., Baumann, R., Kuhn, M., Ström, J., Hagen, D. E., Whitefield, P. D., Baumgardner, D., Arnold, F., Borrmann, S. and Schumann, U. 1997. Near field measurements on contrail properties from fuels with di erent sulfur content. *J. Geophys. Res.* **102**, 29 867–29 880.

Raes, F., Bates, T., McGovern, F. and van Liedekerke, M. 2000. The second aerosol characterization experiment (ACE-2): General context, and main results. *Tellus* **52B**, 111–126.

Randall, D. A., Coakley, J. A. Jr., Fairall, C. W., Kropfli R. A. and Lenschow, D. H. 1984. Outlook for research on subtropical marine stratiform clouds. *Bull. Am. Met. Soc.* **65**, 1290–1301.

Schmeling, M., Russel, L. M., Erlick, C., Collins, D. R., Jonsson, H., Wang, Q., Kregsamer, P. and Streli, C. Aerosol particle chemical characteristics measured from aircraft in the lower troposphere during ACE-2. *Tellus* **52B**, 185–200.

Schröder, F. and Ström, J. 1997. Aircraft measurements of sub micrometer aerosol particles ($>7$ nm) in the midlatitude free troposphere and tropopause region. *Atmos. Research* **44**, 333–356.

Schüller, L., Fischer, J., Armbruster, W. and Bartsch, B. 1997. Calibration of high resolution remote sensing instruments in the visible and near infrared. *Adv. Space. Res.* **19**, 1325–1334.

Snider, J. R. and Brenguier, J. L. 2000. Cloud condensation nuclei and cloud droplet measurements obtained during ACE-2. *Tellus* **52B**, 828–842.

Slingo, A. and Schrecker, H. M. 1982. On the shortwave radiative properties of stratiform water clouds. *Quart. J. Roy. Meteor. Soc.* **108**, 407–426.

Stephens, G. L. and Tsay, S. 1990. On the cloud absorption anomaly. *Quart. J. Roy. Meteor. Soc.* **116**, 671–704.

Twomey, S. 1977. The influence of pollution on the shortwave albedo of clouds. *J. Atmos. Sci.* **34**, 1149–1152.

Twomey, S. and Cocks, T. 1989. Remote sensing of cloud parameters from spectral reflectance measurements in the near-infrared. *Beitr. Phys. Atmos.* **62**, 172–179.

Wood, R., Johnson, D., Osborne, S., Andreae, M. O., Bandy, B., Bates, T., O'Dowd, C., Glantz, P., Noone, K., Quinn, P., Rudolph, J. and Suhre, K. 2000. Boundary layer and aerosol evolution during the third Lagrangian experiment of ACE-2. *Tellus* **52B**, 401–422.